A Planar Broadband Metamaterial Absorber with the Polarization Insensitive and Omnidirectional Absorption in the Min-infrared Regime

Nan Zhang, Linbo Zhang, Guorui Zhang, Peiheng Zhou, Xiaolong Weng, Jianliang Xie, and Longjiang Deng
National Engineering Research Center of Electromagnetic Radiation Control Materials
State Key Laboratory of Electronic Thin Film and Integrated Devices
University of Electronic Science and Technology of China, China

Abstract— In this paper, we present the design, fabrication and characterization of a polarization insensitive and omnidirectional broadband planar metamaterial perfect absorber (MPA) in the min-infrared regime. Multi-sized resonators are employed to excite the broadband absorption, and the absorption bandwidth is efficiently broadened compared with the single-sized absorber. Geometric effects on the resonance wavelengths are studied in detail by using the equivalent circuit model. Experiment result shows that greater than 70% absorption is obtained within a waveband of 0.67 µm, which is in reasonable agreement with the simulation. The electromagnetic response of the MPA is theoretically investigated to reveal the intrinsic absorption mechanism. The broadband planar MPA is polarization insensitive and the absorption retains quite high even at large incident angles. The proposed structure holds promise for many applications, such as sensitive detecting, energy harvesting, and thermal modulating.

1. INTRODUCTION

Metamaterial perfect absorbers (MPAs) have recently gained considerable attention due to their potential applications in research of sensitive sensors [1], solar cells [2], thermal emitters [3], and imaging devices [4, 5]. MPAs are artificially constructed "atoms" that composed of sandwiched multilayers, where the top layer is the metallic resonators separated from the bottom metallic film by a dielectric interlayer. The great absorption works relying on the coupling between metallic components of the sandwiched structure at the resonant frequency. The tunable and controllable effects of MPAs afford them incomparable advantages to the naturally existing materials. Neverthless, for the resonant nature of metamaterials, most MPAs could only absorb the light in a very narrow waveband. Therefore, some efforts have gone into obtaining broadband MPAs by vertically stacking metallic resonators with different geometric dimensions [6, 7]. The complex design and fabrication process, however, have restricted their wide applications in the relevant fields.

In this paper, we design and fabricate a planar broadband metamaterial absorber in the min-infrared regime. Our design approach exhibits significant asvantanges to previous studies [6, 7], which does not need to precisely align metallic resonators between the layers. The absorption bandwidth is effectively broadened by the superposition of all resonances in the multi-sized planar metallic resonators. The proposed broadband MA is polarization insensitive and the absorption magnitude is still very high even at large incident angles for both transverse electric (TE) and transverse magnetic (TM) waves.

2. STRUCTURE DESIGN AND SIMULATIONS SETUP

The designed and fabricated broadband MA is shown in Fig. 1. It consist of a layer of 0.1 µm thick aluminum resonators and a 0.2 µm thick aluminum gound plane, separated by a 0.22 µm thick Al_2O_3 dielectric layer. The metallic resonators are composed of the elaborately arranged rectangular disks in a two-dimensionally symetric structure surrounding the cetral square disks. The period of the planar broadband MA is $P = 4.5\,\mu\text{m}$ for both the x and y directions. The Al resonators have the dimensionally dispersed geometry parameters of $t_1 = 1.7\,\mu\text{m}$, $t_2 = 1.6\,\mu\text{m}$, and $t_3 = 1.5\,\mu\text{m}$.

Numerical simulations were performed with the CST microwave studio [8], which is based on the Finite Integration Time Domain (FITD) algorithm. In the simulations, the dielectric constant (ε_d) of Al_2O_3 is set to 2.28 [9], and the complex permittivity of Al is described by the Drude model with the plasma frequency $\omega_p = 2\pi \times 2895\,\text{THz}$ and the collision frequency $\omega_\gamma = 2\pi \times 15.5\,\text{THz}$ [10]. Periodic boundary conditions were employed for the x-y plane, and a plane wave of TM polarization (with magnetic field H perpendicular to the x-z plane) was normally incident upon the structure as the excitation source. The frequency-dependent absorption was obtained from the S-parameters by $A(\omega) = 1 - T(\omega) - R(\omega) = 1 - |S_{21}|^2 - |S_{11}|^2$, where $T(\omega)$ and $R(\omega)$ are the frequency-dependent transmission and reflection, respectively. Furthermore, because the bottom metallic ground plane with a thickness of 200 nm is thick enough to suppress all the transmission light ($T(\omega) = 0$), the calculation of the absorption could be simplified as $A(\omega) = 1 - R(\omega)$.

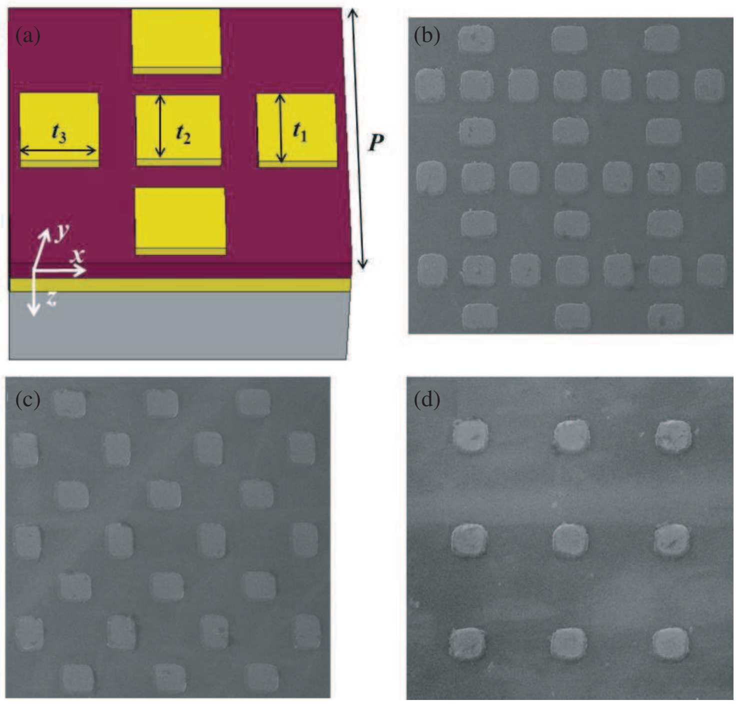

Figure 1: (a) Schematic view of the broadband MPA. Top view SEM images for (b) the structure combined of rectangular and square resonators, (c) the structure composed of separated rectangular resonators, (d) the structure composed of separated square resonators.

3. RESULTS AND DISCUSSIONS

Figure 2(a) shows the simulated absorption spectrum of the present planar broadband MA. It is seen that there are three absorption peaks aroused at 5.73 µm, 5.96 µm, and 6.26 µm with the absorption magnitude of 97.4%, 98.8%, and 98.1%, respectively. Because the high absorption of the three closely positioned resonant peaks, the absorption bandwidth of 97% absorptivity is up to 0.6 µm. To explore the origin of the broadband absorption, absorption spectra for the structures composed of separated rectangular and square resonators were also given in Fig. 2(a). For the structure with rectangular resonators, the absorption peaks of two resonances at 5.70 µm and 6.25 µm are 99.9% and 99.5%, respectively. It is also noted that the absorption bandwidth of 80% absorptivity is 0.88 µm for this structure, and there is a deep dip at 5.98 µm. For the structure with the separated square resonators, the single absorption peak reaonant at 5.91 µm with the 99.5% absorption. We can see that the emergence of the central square resonators compensent the absorption dip in the structure composed of separated rectangular resonators. In other words, by combing these two sperated structures together, the absorption peaks of the two structures are merged into one high absorption broadband spectrum.

Futher exploring of the geometric effects on the resonant behavior of the resonantor are studied in detail by using the equivalent circuit model. It is known that when the light incident upon the MPA structure, antiparallel current will be excited in the metallic resonator and bottom metal ground plane [11]. As a result, an electric current loop emerges. In this sense, one unit cell of the MPA corresponds to a "closed" wire loop. The electric current loop can be mimicked by an LC equivalent circuit model [12]. The resonance absorption is realized when the frequency of the external light equals the eigenfrequency of these resonators. The eigenfrequency of the resonator can be quantitatively described by circuit elements of the LC equivalent circuit model, which depends on the geometrical parameters and dielectric properties of the MPA. Here, we only consider the

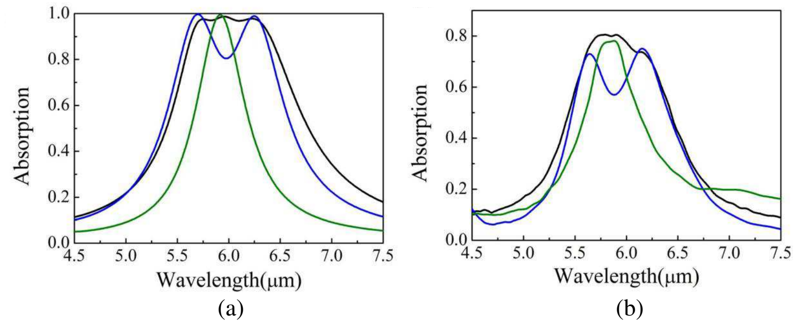

Figure 2: (Color online) (a) Simulated and (b) experimental absorption spectra of the structure combined of rectangular and square resonators (balck line), the structure composed of separated rectangular resonators (blue line), and the structure composed of separated square resonators (green line).

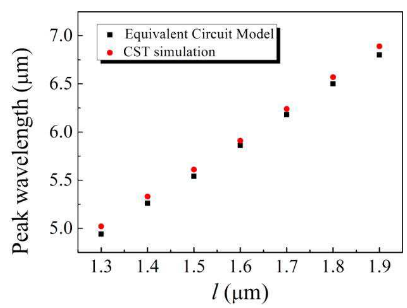

Figure 3: (Color online) Comparison between the predicted peak wavelengths by LC equivalent circuit model and results obtained from the CST simulations for different side length values.

effect of varying the resonator's side length on resonant behavior. The MPA structure discussed in our LC equivalent circuit model is composed of square resonators as the same described in Fig. 1(d) with resonator's side length l varied from 1.3–1.9 μm.

The interaction between the upper resonators and the bottom metallic film can be represented by a parallel plate capacitor of $C_m = \varepsilon_0 \varepsilon_r \sigma_{eff}/d$, and a parallel plate inductor of $L_m = \mu_0 l_{eff} d/(2w)$, where ε_0 is the permittivity of vacuum, ε_r is the real part of the relative permittivity of the Al_2O_3 dielectric layer, σ_{eff} is the effective area of the square resonator where charges spread, d is the thickness of the dielectric layer, μ_0 is the permeability of vacuum, l_{eff} is the effective length in the middle of the square resonator under which most of the magnetic field was trapped. The interaction between the neighboring resonators can be modeled as a gap capacitor of $C_g = 0.5\varepsilon_0 lt/g$, where g is the separate distance of the resonators, and t is the thickness of the resonators. Therefore, total impedance can be expressed as $Z_{tot} = \frac{i\omega L_m}{1-\omega^2 L_m C_g} + \frac{2}{i\omega C_m} + i\omega L_m$, where ω is the angular frequency. Then eigenfrequency ω_r can be deduced from $Z_{tot} = 0$, so $\omega_r = \sqrt{\frac{C_m + C_g - (C_m^2 + C_g^2)^{1/2}}{L_m C_m C_g}}$.

We then calculated the dependence of resonant peak wavelength against the side length l of the square resonator. In Fig. 3, it can be clearly seen that the resonance peak wavelength linearly rises with the increasing of side length l. Moreover, we carried out the numerical simulation for a series of samples with different side length from 1.3 μm to 1.9 μm at the step-width of 0.1 μm. The predicted peak wavelengths are in good agreement with the results indicated by the LC equivalent circuit model. So, for the present planar broadband MA, the long and short side of the rectangular resonator ($t_1 = 1.7$ μm and $t_3 = 1.5$ μm) and the central square resonator ($t_2 = 1.6$ μm) could provide three resonant modes at distinct wavelenths. As a result, the superposition of all these resonances results in the broadband absorption.

To make a better understanding of the broadband absorption mechanism, we investigate the magnetic field distributions at three absorption peaks of the planar broadband MA through numerical simulation. Simulation results (Fig. 4) reveal that magnetic field at 5.73 μm, 5.96 μm, and 6.26 μm are primarily concentrated at the short side of rectangular resonator, the central square resonator and the long side of rectangular resonator, respectively. Magnetic field distributions also verified the prediction of the resonance wavelengths by the LC equivalent circuit model.

In our experiments, electron beam (e-beam) vapor deposition combined with step-and-scan projection lithography techniques were used to prepare the MPAs. A 0.2 μm Al metallic ground plane was first evaporated onto a silicon substrate by e-beam deposition. This was followed by the lithography to define the multiple patterned layers. The 0.22 μm dielectric films and 0.1 μm Al films were then deposited alternately. The pattern transfer was completed by a metal lift-off process. Scanning electron microscopy (SEM) images of the samples are shown in Figs. 1(b)–(d). A Fourier-transform infrared spectrometer (Bruker Vertex 70v) associated with the infrared microscope (Hyperion 2000) was used to measure the reflection spectra. Before measuring, the incident light was calibrated with a gold mirror. The experimentally obtained absorption spectra of the three samples are shown in Fig. 2(b). It is seen that there is a broadband absorption achieving by combining the structures of seperated rectangular and square resonators together, which is in reasonable agreement with the simulation result. The absorption bandwidth of 70% absorptivity is 0.67 μm. Discrepancies between the experimental and simulated results stem from the fabrication tolerance and the inconformity of the dielectric constant of the dielectric spacing layer used in the simulation compared with the actual material parameters.

The absorption performance at non-normal incidence is quite important in practical applications. In many cases, most of possible incident light needs to be absorbed at large incident angles. So we carried out simulations to investigate the angle dependence of the absorber to evaluate its absorption performance at oblique incidence. Fig. 5 shows the absorption spectra as a function of both wavelength and incident angles under TM ($E\perp$ y-z plane) and TE ($E\perp$ x-z plane) polarization. For both configurations, the broadband absorption characteristics can be sustained with increasing the incident angle. However, when the incident angle is appraoch 40°, there is a decrease in the absorption magnitude and a shift in the peak position for the TM polarization waves, and there is a absorption dip for the TE polarization waves. Nevertheless, these simulations reveal that the proposed boradband absorber operates quite well for both TE and TM polarizations over a wide range of incident angles.

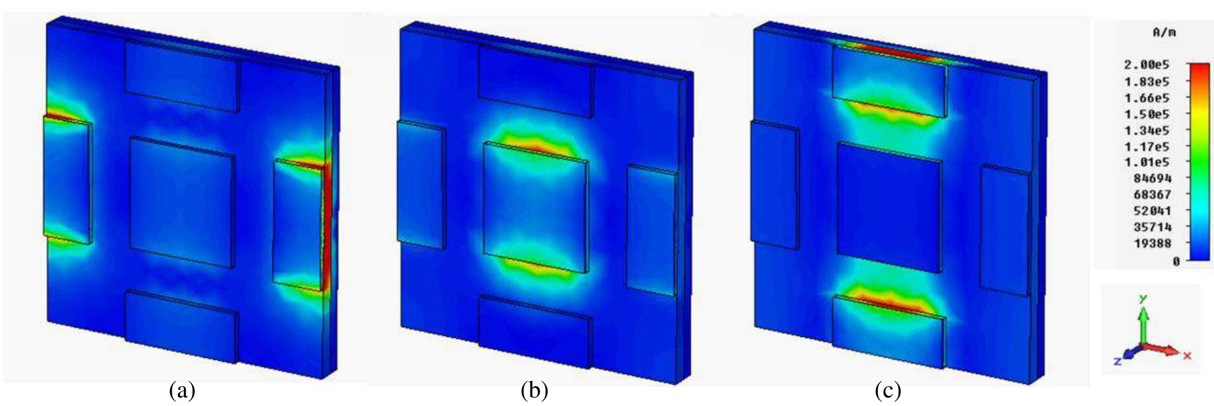

Figure 4: (Color online) Magnetic field distributions at absorption peaks of (a) 5.73 μm, (b) 5.96 μm, (c) 6.26 μm. (There are only half of the short side of rectangular resonator in the given field distributions, for the symmetry setup of the structure in the simualtion).

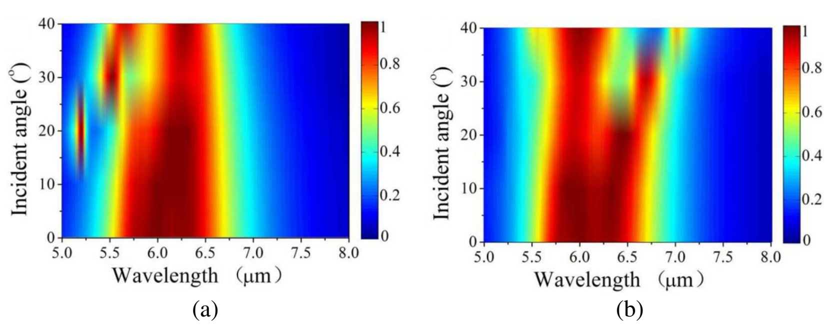

Figure 5: (Color online) Absorbance as a function of wavelength and the angle of incidence for (a) TM and (b) TE polarization incident light.

4. CONCLUSIONS

In conclusion, we have present a planar metamaterial perfect absorber worked in the min-infrared regime, which is polarization insensitive and the absorption is still high even at large incident angles. The broadband absorption originates from the superposition of multiple resonances of the multi-sized resonators. The presented design approach does not need to precisely align metallic resonators between the layers, and could simplify the fabrication process. The proposed structure may have multiple application values in the relevant fields, such as sensitive detecting, energy harvesting, and thermal modulating.

REFERENCES

1. Liu, N., M. Mesch, T. Weiss, M. Hentschel, and H. Giessen, "Infrared perfect absorber and its application as plasmonic sensor," *Nano Lett.*, Vol. 10, 2342, 2010.
2. Wang, Y., T. Sun, T. Paudel, Y. Zhang, Z. Ren, and K. Kempa, "Metamaterial-plasmonic absorber structure for high efficiency amorphous silicon solar cells," *Nano Lett.*, Vol. 12, 440, 2011.
3. Liu, X., T. Tyler, T. Starr, A. F. Starr, N. M. Jokerst, and W. J. Padilla, "Taming the blackbody with infrared metamaterials as selective thermal emitters," *Phys. Rev. Lett.*, Vol. 107, 045901, 2011.
4. Mason, J. A., S. Smith, and D. Wasserman, "Strong absorption and selective thermal emission from a midinfrared metamaterial," *Appl. Phys. Lett.*, Vol. 98, 241105, 2011.
5. Liu, X., T. Starr, A. F. Starr, and W. J. Padilla, "Infrared spatial and frequency selective metamaterial with near-unity absorbance," *Phys. Rev. Lett.*, Vol. 104, 207403, 2010.
6. Ye, Y. Q., Y. Jin, and S. He, "Omnidirectional, polarization-insensitive and broadband thin absorber in the terahertz regime," *J. Opt. Soc. Am. B*, Vol. 27, 498, 2010.
7. Grant, J., Y. Ma, S. Saha, A. Khalid, and D. R. S. Cumming, "Polarization insensitive, broadband terahertz metamaterial absorber," *Opt. Lett.*, Vol. 36, 3476, 2011.
8. CST Microwave Studio 2009, (Computer Simulation Technology GmbH, Darmstadt, Germany).
9. Palik, E. D., *Handbook of Optical Constants in Solids*, Academic Press, 1991.
10. Ordal, M. A., L. L. Long, R. J. Bell, S. E. Bell, R. R. Bell, R. W. Alexander, Jr., and C. A. Ward, "Optical properties of the metals Al, Co, Cu, Au, Fe, Pb, Ni, Pd, Pt, Ag, Ti, and W in the infrared and far infrared," *Appl. Opt.*, Vol. 22, 1099, 1983.
11. Liu, N., M. Mesch, T. Weiss, M. Hentschel, and H. Giessen, "Infrared perfect absorber and its application as plasmonic sensor," *Nano Lett.*, Vol. 10, 2342, 2010.
12. Cheng, D., J. Xie, H. Zhang, C. Wang. N. Zhang, and L. Deng, "Pantoscopic and polarization-insensitive perfect absorbers in the middle infrared spectrum," *J. Opt. Soc. Am. B*, Vol. 29, 1503, 2012.